# Propagation of shear bands in a $Cu_{47.5}Zr_{47.5}Al_5$ bulk metallic glass

K.B. Kim[a)]

*Faculty of Nanotechnology and Advanced Materials Engineering, Sejong University, Gwangjin-gu, Seoul 143-747, Korea*

J. Das and M.H. Lee

*Leibniz Institute for Solid State and Materials Research (IFW) Dresden, Institute for Complex Materials, Dresden D-01171, Germany*

S. Yi

*Department of Materials Sciences and Metallurgy, Kyungpook National University, Buk-gu, Daegu 702-701, Korea*

E. Fleury

*Advanced Metals Research Center, Korea Institute of Sciences and Technology, Cheongryang, Seoul 130-650, South Korea*

Z.F. Zhang

*Shenyang National Laboratory for Materials Science, Institute of Metal Research, Chinese Academy of Sciences, Shenyang 110016, China*

W.H. Wang

*Institute of Physics, Chinese Academy of Sciences, Beijing 100080, China*

J. Eckert[b)]

*Leibniz Institute for Solid State and Materials Research (IFW) Dresden, Institute for Complex Materials, Dresden D-01171, Germany*

We report a novel finding of slither propagation of shear bands on the fracture surface of a $Cu_{47.5}Zr_{47.5}Al_5$ bulk metallic glass (BMG). The nanoscale heterogeneities in the as-cast state are aggregated along shear bands with irregular morphology. Such heterogeneities create a fluctuating stress field during shear band propagation leading to a slither propagation mode. The slither propagation of 10 to 15 nm wide shear bands is effective to improve both the plasticity and the "work-hardening-like" behavior of BMGs if the size, the morphology, and the elastic properties of the heterogeneities are intimately intercalated during solidification.

## I. INTRODUCTION

Bulk metallic glasses (BMGs) usually undergo inhomogeneous plastic deformation at room temperature with very limited macroscopic plastic strain.[1–4] The plastic flow allows only a few shear bands to be active, causing catastrophic failure of the sample.[1–4] This disadvantage of BMGs creates a significant difficulty for its use in industrial applications. The recent development of unique BMGs, so-called ductile BMGs, overcoming this disadvantage, has been highlighted in several publications.[5–10] Consequently, it is an urgent issue to understand the deformation mechanisms of these ductile BMGs. So far, there are two major trends attempting to solve the deformation mechanisms operating in ductile BMGs: the first approach considers the elastic constants of the material,[7,9,11] and the second one focuses on microstructural heterogeneities.[5,6,8,10,12] The flow of metallic glass-forming liquids, and the flow and fracture of metallic glasses and their relation to elastic constants, i.e., Poisson's ratio $\nu$, have been used to determine the ductility or brittleness of BMGs.[7,11] Similarly, the intrinsic plasticity and brittleness of BMGs have also been correlated with the ratio of the elastic shear modulus $\mu$ to the bulk modulus $B$,[9,13] based on the known database. Indeed, this approach is very helpful to make an overall sketch for designing and understanding the plasticity of

BMGs. However, just considering these critical values is too simple to fully understand the ductility of BMGs within the "real" amorphous structure, which can be as a rough first approximation described as an open structure of randomly distributed atoms with topological or chemical short range order[4] including of structural inhomogeneities[8] (i.e., phase separation,[12] medium-range order).[5,8] In other words, the material can exhibit a large degree of heterogeneity. Accordingly, another approach comes from considering microstructural heterogeneities, i.e., structural[6,10] and chemical fluctuations.[5,8] The heterogeneity of BMGs can play an important role for the nucleation of shear bands and thus also governs the multiplication of shear bands.[8] Furthermore, some extended ideas are linked with the occurrence of mechanically induced nanocrystallization[14] and agglomeration,[15] as well as phase separation[16] during the propagation of shear bands. Although most of the previous investigations are plausible, these concepts are not fully suitable to elucidate the very recent discovery of work-hardening-like behavior in ductile BMGs, developed by a small compositional tuning, i.e., the introduction of Sn[17] and Al,[8] starting from equiatomic binary $Ti_{50}Cu_{50}$ and $Zr_{50}Cu_{50}$ alloys.

In the present investigation, we report on the slither propagation of shear bands observed at the edge of the fracture surface in a $Cu_{47.5}Zr_{47.5}Al_5$ BMG. Systematic microstructural investigations of the as-cast microstructure reveal that the glass contains nanoscale chemical heterogeneities with spherical morphology and 10 to 20 nm in size.[12] Moreover, there is also a macroscopic heterogeneity that can be distinguished from the different degree of the chemical fluctuations in the sample, and the existence of nanoscale crystals of less than 5 nm in size.[12] Microstructural analysis of the fracture surface reveals a strong aggregation and interaction of the nanoscale chemical heterogeneity along the slither shear band propagation. In contrast, the propagation of shear bands in the areas containing nanocrystals, i.e., macroscopic heterogeneous areas, is quite thick and straight.[18] So far there have been no detailed investigations based on the interaction of the different motions of the shear bands to fully understand the deformation mechanism of the $Cu_{47.5}Zr_{47.5}Al_5$ BMG. As a first step, the slither propagation of shear bands can be incorporated in a model description attempting to understand both the ductility and the "work-hardening-like" behavior in the $Cu_{47.5}Zr_{47.5}Al_5$ BMG in terms of local stress and strain instabilities.

## II. EXPERIMENTAL

The $Cu_{47.5}Zr_{47.5}Al_5$ alloy was prepared by arc melting the pure elements under an argon atmosphere and direct casting into cylindrical rods with 2 mm diameter using an in situ suction casting facility, attached to the arc melter.

Phase analysis was done by x-ray diffraction (XRD) with Cu $K_\alpha$ radiation. Detailed structural investigations of the as-cast samples were performed by high-resolution transmission electron microscopy (HRTEM) coupled with energy-dispersive x-ray analysis (EDX). Thin slices have been prepared from the as-cast and deformed specimens after fracture. The TEM specimens were prepared by the conventional method of slicing and grinding, followed by ion milling with liquid nitrogen cooling.

## III. RESULTS AND DISCUSSION

From the stress–strain curves under uniaxial compressive load (at an initial strain rate of $8 \times 10^{-4}$ $s^{-1}$ at room temperature) the mechanical properties of the $Cu_{47.5}Zr_{47.5}Al_5$ BMG have been investigated (for further details, see Ref. 8). The values of Young's modulus $E$, yield stress $\sigma_y$, yield strain $\epsilon_y$, ultimate compression stress $\sigma_{max}$, and fracture strain $\epsilon_f$ are 87 GPa, 1547 MPa, 2.0%, 2265 MPa, and 18.0%, respectively. During compression, the specimens first buckle, then fracture.[8] The calculated true stress–strain curve from the engineering stress–strain data reveals a stress increase with further increasing strain as is typical for work hardening. The stress increases from 1547 to 1865 MPa, as determined from the true stress–strain curve. The Poisson's ratio $\nu$, the shear modulus $G$, and the bulk modulus $B$ obtained from ultrasonic measurements are 0.365, 33.0, and 113.7 GPa, respectively. A large number of shear bands are also observed on the fracture surface of the specimen. However, the observed shear bands are quite wavy in nature,[8] and their spacing is 150 to 500 nm, revealing a high density of shear band formation. Moreover, one can find interactions of the shear bands on the fracture surface indicating a macroscopically homogeneous nucleation and distribution of the shear bands throughout the sample to accommodate the applied strain.

Figure 1 shows a TEM bright-field image (a), a selected-area diffraction (SAD) pattern (b), and a HRTEM image (c) of the as-cast $Cu_{47.5}Zr_{47.5}Al_5$ BMG. The TEM bright-field image reveals a unique microstructure, consisting of a homogeneous distribution of regions with spherical dark contrast in a bright contrast matrix. The size of the spherical dark contrast is about 5 to 15 nm. The SAD pattern in Fig. 1(b) displays halo diffraction intensities, i.e., typical amorphous characteristics. Chemical analysis using conversion nanobeam EDX with a spot size of ~7 nm in diameter reveals that the dark contrast areas in Fig. 1(a) contain high Cu and poor Zr content compared with the bright contrast areas. The HRTEM image in Fig. 1(c) clearly reveals the areas with bright and dark contrast, as indicated by the arrow. The size of the spherical dark contrast areas of about 5 to 15 nm is similar as in Fig. 1(a). In neither the bright nor the dark contrast areas, can one find any indication of
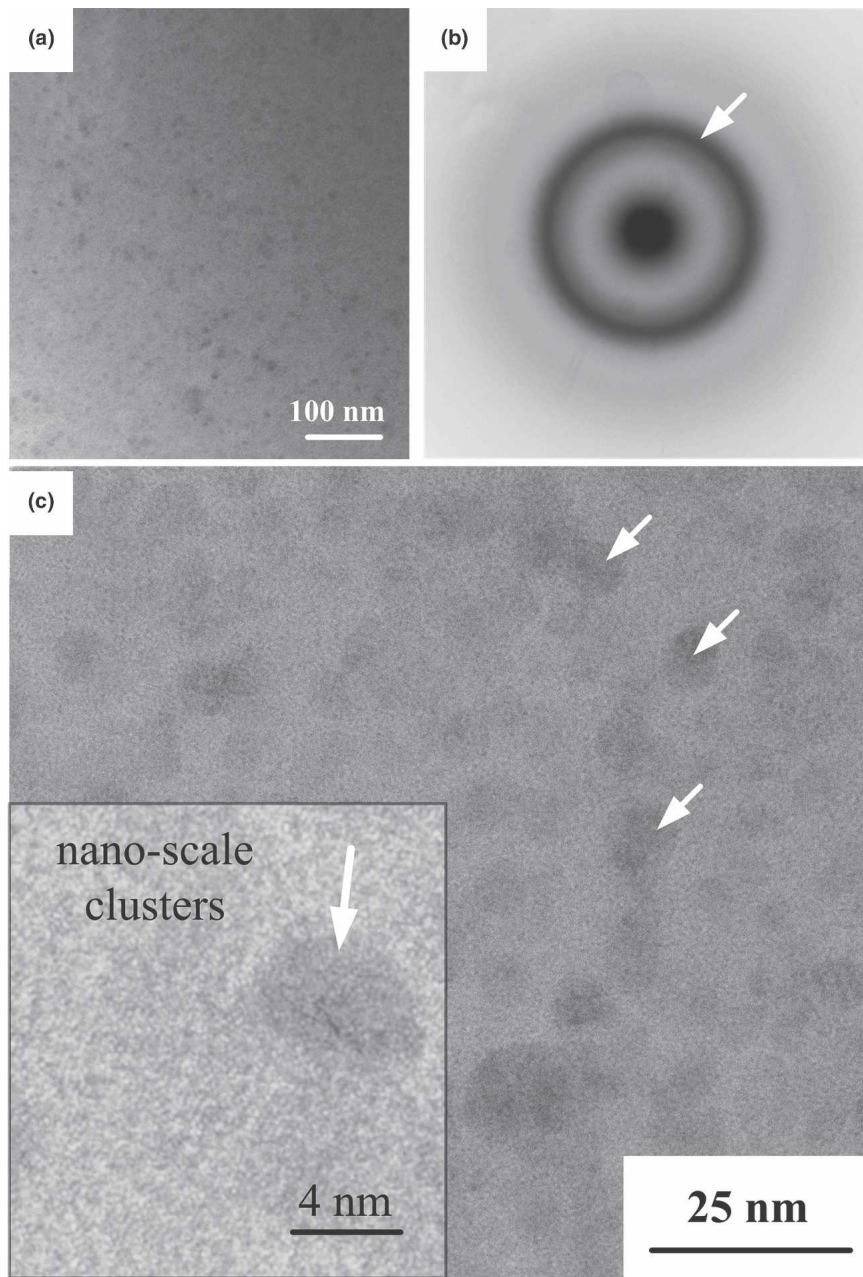
FIG. 1. As-cast Cu$_{47.5}$Zr$_{47.5}$Al$_5$ BMG. (a) TEM bright-field image. (b) SAD pattern. (c) HRTEM images.

regular lattice fringes confirming the formation of an amorphous structure in this glassy alloy.

Figure 2 shows a TEM bright-field image (a), a SAD pattern (b), and a HTREM image obtained from the edge areas of the fracture surface of the deformed Cu$_{47.5}$Zr$_{47.5}$Al$_5$ BMG. The TEM bright-field image clearly shows the slither propagation mode of a shear band. The width of the shear band is estimated to be 10 to 15 nm as measured from the high-resolution images. However, the width of the slither shear band gradually decreases, indicating there may be a significant decrease of strain during the propagation. The half wavelength

($\lambda/2$) of such slither propagation of shear bands varies between 60 and 128 nm. One can find a significant agglomeration of clusters of the dark contrast along the slither shear bands, as indicated by dotted circles. This indicates that the distribution of the nano-scale heterogeneous areas tends to become agglomerated locally along the shear bands rather than being homogeneously distributed as in the as-cast microstructure [Figs. 1(a) and 1(c)]. The SAD pattern in Fig. 2(b) reveals halo diffraction intensities, similar to those in the as-cast sample [Fig. 1(b)]. This indicates that there is no mechanically induced phase transformation, i.e.,
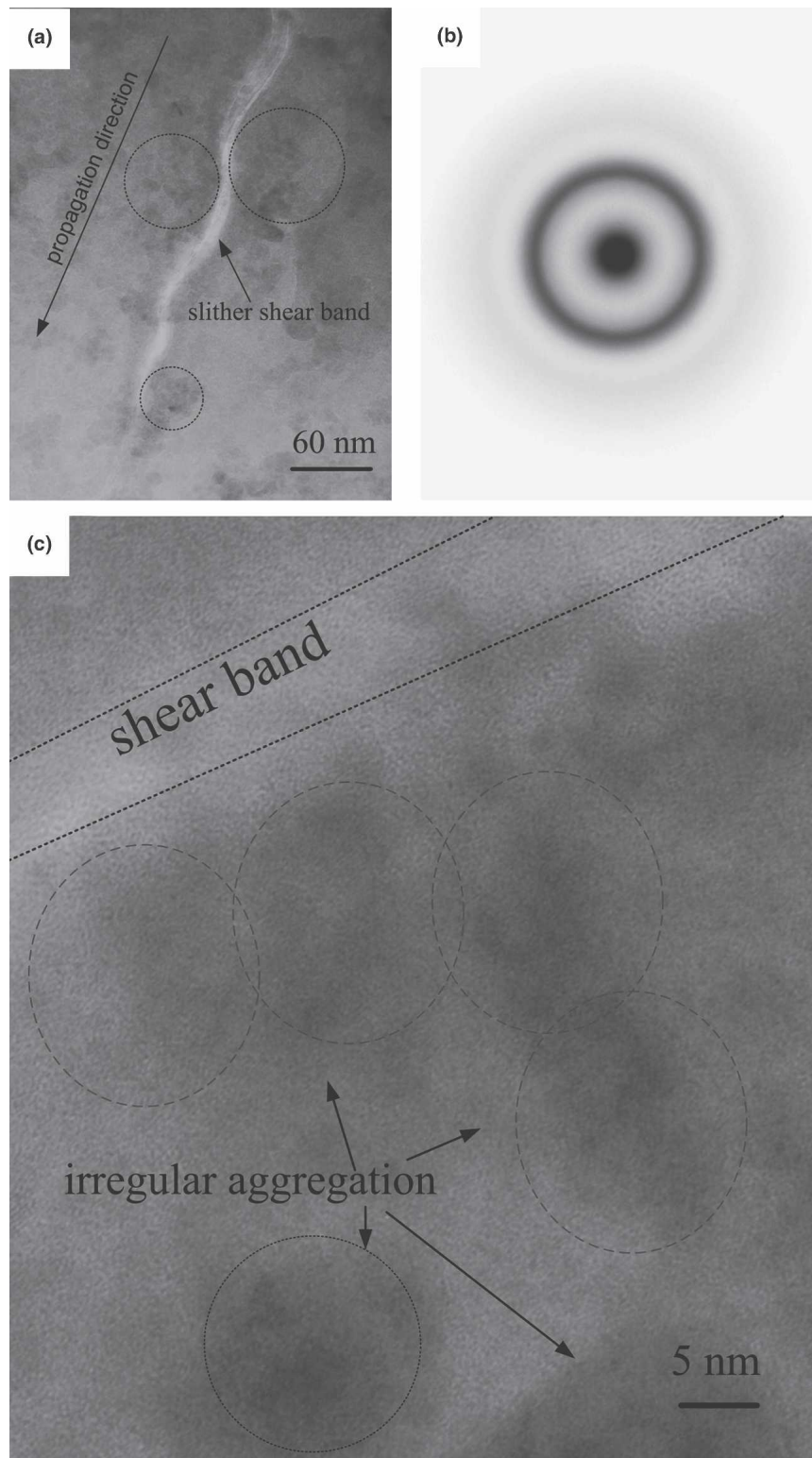
FIG. 2. Deformed $Cu_{47.5}Zr_{47.5}Al_5$ BMG. (a) TEM bright-field image. (b) SAD pattern. (c) HRTEM images.

nanocrystallization. The HRTEM image in Fig. 2(c) also reveals that no regular lattice fringes are present through-out the sample, confirming that there is no crystalline phase. However, the areas with dark contrast are highly clustered along the shear bands, as indicated by dot-circles. Furthermore, the morphology of the aggregated areas with the dark contrast is highly irregular rather than spherical as in the as-cast state [Fig. 1]. Comparing these

findings with the as-cast microstructure [Fig. 1(a) and 1(c)] suggests that a strong aggregation and a local rearrangement of heterogeneous areas occur by the interactions to the shear bands.

The aggregation of the nanoscale heterogeneity along the shear bands is presumably caused by an effect of a vortex.[19] Since it has been known that shear bands contain a high concentration of free volume,[1] local density differences between the inner and outer areas of the shear bands may occur. As described in Fig. 2, the irregular interfaces linked with aggregation of the nanoscale heterogeneity suggest that there is significant rotation of the aggregates. Therefore, it is very likely possible to develop an inhomogeneous clustering of the nanoscale heterogeneous areas, thus providing continuous local differences in shear stress and strain during the propagation of the shear bands. Similar interactions of the nanoscale heterogeneities during deformation have been reported for various types of viscous materials: low-viscosity material (e.g., a complex fluid with micelles, showing inhomogeneous flow[20]), as well as relatively highly viscous materials (e.g., a polymer–nanoparticle composite forming crazes at the crack tips[21]). For the inhomogeneous flows in miscellaneous complex fluids, it is well known that an applied shear stress can generate two stable shear strain rates, producing a flow instability.[20] In contrast, the crazes in polymer materials during deformation require a significant local distortion of the atomic bonds, based on the chain clustering.[21] Hence, the local medium-range order along the propagating shear bands can be modified from the original state after the deformation of these materials.

Recent suggestions to understand the flow and fracture of metallic glasses with a relationship to elastic constants[7,9,11,13] can also be an important factor to elucidate the slither movement of the shear bands in the present investigation. However, as we described previously, there are two amorphous phases upon solidification, i.e., A and A′. Hence, the overall Young's modulus should be considered $E_{overall} = X_A \times E_A + X_{A'} \times E_{A'}$, where $X_A$, $X_{A'}$, $E_{overall}$, $E_A$, and $E_{A'}$ are the volume fraction of the phase A and A′, the experimentally determined overall Young's modulus $E_{overall}$ of the material, and the Young's moduli $E_A$ and $E_{A'}$ for the phases A and A′. Similar considerations will hold for all elastic constants. In this sense, the mechanical behavior of the Cu$_{47.5}$Zr$_{47.5}$Al$_5$ BMG cannot be directly correlated to simple criteria, as determined by values such as Poisson's ratio[7,11] and the ratio of the elastic shear modulus μ to the bulk modulus $B$,[9,13] which were developed to interpret the ductile-brittle transition in metallic glasses.

The morphology and the distribution of the nanoscale heterogeneity should be important during the deformation. Of course, an understanding of how to enhance the ductility and work hardenability of BMGs can be par-

tially satisfied with the previously considered nanocrystals incorporated in the amorphous matrix.[6,10] From the previous investigations on dynamic nanocrystallization[14] and aggregation of pre-existing nanocrystals[15] in some ductile BMGs, both contributions can be effective ways to understand the enhancement of the plasticity. This can be understood from the schematic representation of the clustered glassy structure as described in Fig 3. During propagation of 10 to 15 nm wide shear bands, there exists a local elastoplastic coupling-induced elastic anisotropy, which may evolve due to reorientation of the nanoscale heterogeneity, modification of the intercluster contacts, and their subsequent annihilation/disordering. This may degrade the local elastic stiffness and assists wavy propagation of the shear bands. Most likely the propagation of the shear bands also destroys/disorders at least some clusters inside the bands. As is well known for honeycomb structures, the presence of an oscillating stress field[22] creates dynamic disturbances to the shear bands enhancing their slither propagation.

The former observations on the structural features of shear bands formed in monolithic bulk metallic glass and glassy ribbons[23,24] are significantly different from what was observed in the present study. According to the free-volume theory[1,23] and the bubble raft mechanism,[25] coalescence of excess free volume in a shear band continuously increases the defect density leading to nanovoids[23] and induces the nucleation of cracks. However, the elastic nature of a volume element in front of a shear band must be crucial to determine its structural features and propagation pathway. It is well known that shearing events and local rearrangement of a group of atoms [shear transition zone, (STZ)] under an applied stress leads to plastic yielding and an inhomogeneous deformation at room temperature. A further increment of stress rapidly activates a large numbers of STZs, leading to interconnection between them to form shear bands.[15] In this process, the interaction between the STZs in monolithic metallic glass are almost neglected [Fig. 3(c)]. However, the unstable STZs are prone to initiate cleavage. The presence of structural inhomogeneities (structures with different elastic properties) leads to an interaction between the STZs at different regions.[26] This may, in turn, lead to a stress oscillation determining the slither mode of shear band propagation. The decrease in the wavelength [Figs. 2(a), 3(b), 3(c); $L_A = 128$ nm, $L_B = 60$ nm] and the width of the shear band into the propagation direction indicate a further requirement of the shear stress for driving the shear bands. The wavy feature helps to increase the surface area and dissipate the accumulated energy of the shear bands.

## IV. SUMMARY

The novel finding of slither propagation of shear bands has been observed on the fracture surface of a
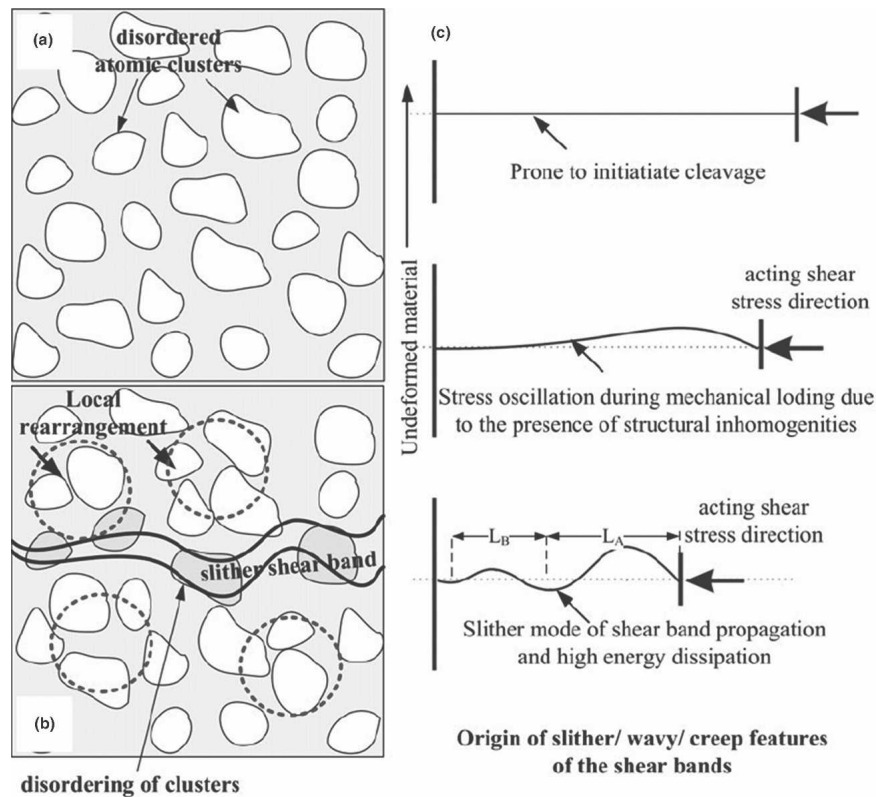
FIG. 3. Clustered glassy structure (a) before, and (b) after shear band propagation showing the local agglomeration of clusters outside the shear band and annihilation/disordering of clusters inside the shear band. (c) The variation of the stress amplitude and stress oscillation in nanoscopic scale caused by structural inhomogeneities in metallic glass drives the slither mode of shear band propagation.

"work-hardenable" ductile $Cu_{47.5}Zr_{47.5}Al_5$ BMG. This finding possibly opens new approaches to understand the emerging plasticity and "work-hardening-like" behavior of BMGs. The slither shear band propagation is considered to be due to local stress–strain differences caused by the interaction of the shear band with a nanoscaleheterogeneity, which as a result, leads to aggregation of the heterogeneous areas along the shear bands.

## REFERENCES

1. F. Spaepen: Microscopic mechanism for steady-state inhomogeneous flow in metallic glasses. *Acta Metall.* **25,** 407 (1977).
2. A.S. Argon: Plastic deformation in metallic glasses. *Acta Metall.* **27,** 47 (1979).
3. A.L. Greer: Metallic glasses. *Science* **267,** 1947 (1995).
4. W.L. Johnson: Bulk glass-forming metallic alloys: Science and technology. *MRS Bull.* **24,** 42 (1999).
5. L.Q. Xing, Y. Li, K.T. Ramesh, J. Li, and T.C. Hufnagel: Enhanced plastic strain in Zr-based bulk amorphous alloys. *Phys. Rev. B* **64,** 180201 (2001).
6. A. Inoue, W. Zhang, T. Zhang, and K. Kurosaka: High-strength Cu-based bulk glassy alloys in Cu–Zr–Ti and Cu–Hf–Ti ternary systems. *Acta Mater.* **49,** 2645 (2001).
7. J. Schroers and W.L. Johnson: Ductile bulk metallic glass. *Phys. Rev. Lett.* **93,** 255506 (2004).
8. J. Das, M.B. Tang, K.B. Kim, R. Theissmann, F. Baier, W.H. Wang, and J. Eckert: "Work-hardenable" ductile bulk metallic glass. *Phys. Rev. Lett.* **94,** 205501 (2005).
9. X.K. Xi, D.Q. Zhao, M.X. Pan, W.H. Wang, Y. Wu, and J.J. Lewandowski: Fracture of brittle metallic glasses: brittleness or plasticity. *Phys. Rev. Lett.* **94,** 125510 (2005).
10. H. Kato, A. Inoue, and J. Saida: Influence of hydrostatic pressure during casting on as cast structure and mechanical properties in $Zr_{65}Al_{7.5}Ni_{10}Cu_{17.5-x}Pd_x$ ($x$ = 0, 17.5) alloys. *Scripta Mater.* **51,** 1063 (2004).
11. W.L. Johnson and K. Samwer: A universal criterion for plastic yielding of metallic glasses with a $(T/T_g)^{2/3}$ temperature dependence. *Phys. Rev. Lett.* **95,** 195501 (2005).
12. K.B. Kim, J. Das, S. Venkataraman, S. Yi, and J. Eckert: Work

hardening ability of ductile $Ti_{45}Cu_{40}Ni_{7.5}Zr_5Sn_{2.5}$ and $Cu_{47.5}Zr_{47.5}Al_5$ bulk metallic glasses. *Appl. Phys. Lett.* **89,** 071908 (2006).

13. J.J. Lewandowski, W.H. Wang, and A.L. Greer: Intrinsic plasticity or brittleness of metallic glasses. *Philos. Mag. Lett.* **85,** 77 (2005).

14. J. Saida, A.D. Setyawan, H. Kato, and A. Inoue: Nanoscale multistep shear band formation by deformation-induced nanocrystallization in Zr–Al–Ni–Pd bulk metallic glass. *Appl. Phys. Lett.* **87,** 151907 (2005).

15. A. Inoue, W. Zhang, T. Tsurui, A.R. Yavari, and A.L. Greer: Unusual room-temperature compressive plasticity in nanocrystal-toughened bulk copper-zirconium glass. *Philos. Mag. Lett.* **85,** 221 (2005).

16. Q. Cao, J. Li, Y. Zhou, and J.Z. Jiang: Mechanically driven phase separation and corresponding microhardness change in $Cu_{60}Zr_{20}Ti_{20}$ bulk metallic glass. *Appl. Phys. Lett.* **86,** 081913 (2005).

17. K.B. Kim, J. Das, X.D. Wang, Z.F. Zhang, J. Eckert, and S. Yi: Effect of Sn on microstructure and mechanical properties of (Ti-Cu)-based bulk metallic glasses. *Philos. Mag. Lett.* **86,** 479 (2006).

18. K.B. Kim, J. Das, and J. Eckert: unpublished works.

19. D.M. Mueth, G.F. Debregeas, G.S. Karczmar, P.J. Eng, S.R. Nagel, and H.M. Jaeger: Signatures of granular microstructure in dense shear flows. *Nature* **406,** 385 (2000).

20. G. Porte, J-F. Berret, and J.L. Harden: Inhomogeneous flows of complex fluids: Mechanical instability versus non-equilibrium phase transition. *J. Phys. II France* **7,** 459 (1997).

21. J. Tung, R.K. Gupta, G.P. Simon, G.H. Edward, and S.N. Bhattacharya: Rheological and mechanical comparative study of in situ polymerized and melt-blended nylon 6 nanocomposites. *Polymer* **46,** 10405 (2005).

22. S.D. Papka and S. Kyriakides: Biaxial crushing of honeycombs: Part 1. *Exp. Int. J. Solids Struct.* **36,** 4367 (1999).

23. J. Li, F. Spaepen, and T.C. Hufnagel: Nano-scale defects in shear bands in a metallic glass. *Philos. Mag. A* **82,** 2623 (2002).

24. P.E. Donovan and W.M. Stobbs: The structure of shear bands in metallic glasses. *Acta Metall.* **29,** 1419 (1981).

25. A.S. Argon: Mechanisms of inelastic deformation in metallic glasses. *J. Phys. Chem. Solids* **43,** 945 (1982).

26. J. Das, K.B. Kim, W. Xu, B.C. Wei, Z.F. Zhang, W.H. Wang, S. Yi, and J. Eckert: Ductile metallic glasses in supercooled martensitic alloys. *Mater. Trans.* **37,** 2606 (2006).

12

J. Mater. Res., Vol. 23, No. 1, Jan 2008